UNIVERSITY *of* York

This is a repository copy of *Rapid and accurate broadband absorption cross-section measurement of human bodies in a reverberation chamber*.

White Rose Research Online URL for this paper:
https://eprints.whiterose.ac.uk/86264/

Version: Accepted Version

Article:

Flintoft, Ian David orcid.org/0000-0003-3153-8447, Melia, Gregory Connor Richard, Robinson, Martin Paul orcid.org/0000-0003-1767-5541 et al. (2 more authors) (2015) Rapid and accurate broadband absorption cross-section measurement of human bodies in a reverberation chamber. Measurement Science and Technology. 065701. ISSN 0957-0233

https://doi.org/10.1088/0957-0233/26/6/065701

White Rose
university consortium
Universities of Leeds, Sheffield & York

eprints@whiterose.ac.uk
https://eprints.whiterose.ac.uk/

Rapid and accurate broadband absorption cross-section measurement of human bodies in a reverberation chamber

Ian D Flintoft[1], Gregory C R Melia[2], Martin P Robinson[1], John F Dawson[1] and Andy C Marvin[1]

[1] Department of Electronics, University of York, Heslington, York YO10 5DD, UK
[2] Medical Physics Department, Freeman Hospital, Newcastle upon Tyne NE7 7DN, UK

Statement of Provenance

Rapid and Accurate Broadband Absorption Cross-Section Measurement of Human Bodies in a Reverberation Chamber

Ian D. Flintoft, Gregory C. R. Melia, Martin P. Robinson,

John F. Dawson and Andy C. Marvin

Abstract—**A measurement methodology for polarisation and angle of incidence averaged electromagnetic absorption cross-section using a reverberation chamber is presented. The method is optimised for simultaneous rapid and accurate determination of average absorption cross-section over the frequency range 1 to 15 GHz, making it suitable for use in human absorption and exposure studies. The typical measurement time of the subject is about eight minutes with a corresponding statistical uncertainty of about 3% in the measured absorption cross-section. The method is validated by comparing measurements on a spherical phantom with Mie Series calculations. The efficacy of the method is demonstrated with measurements of the posture dependence of the absorption cross-section of a human subject and an investigation of the effects of clothing on the measured absorption which are important considerations for the practical design of experiments for studies on human subjects.**

Index Terms—**Absorption cross-section, reverberation chamber, whole body specific absorption rate**

1   INTRODUCTION

The measurement of the electromagnetic absorption cross-section (ACS) of human subjects is required for a number of applications which include the estimation of the effects of human subjects on electromagnetic wave propagation used for communications in structures such as airframes and other vehicles, biometrics and safety-related electromagnetic exposure studies. All these applications are stochastic in nature, thus a stochastic method is appropriate for their measurement. The work presented in this paper extends the well-known technique described by Carlberg *et al* [1] and Gifuni *et al* [2] by optimizing the measurement for use in studies on human subjects. Similar work on in-situ exposure measurements has been partially described for airframe measurement applications [3] and in-situ exposure assessment using room electromagnetics [4]. In these approaches direct non-stochastic coupling occurs between the antennas and the subject which introduces systematic uncertainties into the measured ACS. Here we use a metrological reverberation chamber and analyse these systematic effects in detail in order to minimize the uncertainty.

The limitations imposed on the measurements by the human subjects are critical in informing the experimental design. The ACS of a human subject is dependent on the posture adopted. To fully understand the range of ACS obtained through posture variation it is necessary for the subjects to adopt the postures concerned (standing, seated, foetal, etc.) for the whole measurement
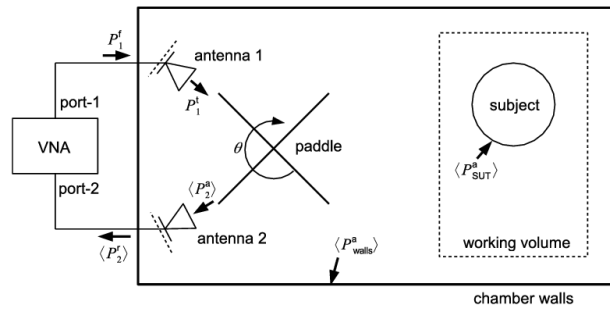
Fig. 1.   Plan view of the experimental configuration for human ACS measurements in a reverberation chamber.   The dashed lines indicated the calibration planes of the VNA.

time. Subjects may not be able to hold some of these postures over extended time periods and any movement of the subjects will add to the measurement uncertainty. In previous work we used a technique based on stepped mechanical tuning to study the loading effect of people in airframes for electromagnetic compatibility purposes [5]. As will be demonstrated, this technique is not suitable for applications requiring discrimination between subjects, due to limited accuracy and long measurement times. For this reason the ACS measurement technique we describe has been optimised for minimum measurement time whilst improving the accuracy required for such applications. A wide frequency range is also advantageous and should be covered in a single measurement of the subject. The ICNIRP restrictions on whole-body SAR cover the range 100 kHz to 10 GHz [6], while there are many mobile communication systems with operating frequencies from 1-5 GHz. Here we present measurements in the 1 GHz to 15 GHz frequency range, a range determined by the limitations of the reverberation chamber available. In principle the frequency range could be extended beyond this range in a suitable chamber given the constraints described below.

The method described has been validated on a spherical shell filled with distilled water using an accurate Mie series calculation which has also been used to examine the associated error model [7]. Human ACS measurements with seated, foetal and star postures are presented and the effects of differing amounts of clothing are also demonstrated. These measurements were not designed as a systematic study of exposure, but rather to assess the potential systematic uncertainties due to posture changes during the measurement and the extent to which clothing affects the measurement. The quantification of these effects is important for informing the design of human volunteer experiments.

2   MEASUREMENT THEORY AND EXPERIMENTAL DESIGN

2.1   ACS measurement in a reverberation chamber

The experimental arrangement for measuring ACS in a reverberation chamber is shown in Fig. 1. The chamber used in this study has dimensions $4.70 \text{ m} \times 3.00 \text{ m} \times 2.37 \text{ m}$ and has a paddle for mechanical tuning of the cavity modes driven by a computer-controlled stepper motor in the roof. Two broadband double ridged waveguide horn antennas are located inside the chamber such that they do not directly illuminate the subject and do not have a direct line of sight between their main beams. The transmission between the antennas is measured using a vector network analyser (VNA). The subject-under-test (SUT) must be located more than a quarter-wavelength from the walls of the chamber and the paddle at the lowest frequency of the measurement, which defines the working volume of the chamber.

The measurement operates by averaging the transmission between the antennas over an ensemble of independent field configurations obtained by tuning the cavity modes. Such average quantities are denoted by $\langle \ldots \rangle$. The tuning randomises the multiple reflections in the chamber and results in an average field at any point which is equivalent to that from an infinite set of plane waves arriving from all directions and with all polarizations [8].

The total average power absorbed due to all the loss mechanisms in the reverberation chamber, $\langle P^a \rangle$, and hence the total absorption cross-section $\langle \sigma_T^a \rangle$, can be written as a sum of partial cross-sections, $\langle \sigma_i^a \rangle$, due to each loss mechanism [8]:

$$\langle P^{\mathrm{a}} \rangle = \langle S \rangle \sum_i \langle \sigma_i^{\mathrm{a}} \rangle = \langle S \rangle \langle \sigma_{\mathrm{T}}^{a} \rangle, \tag{1}$$

where $\langle S \rangle$ is the average power density. Each partial cross-section can also written in terms of a partial Q-factor, $\langle Q_i \rangle = \omega \langle U \rangle / \langle P_i^{\mathrm{a}} \rangle$, where ω is the angular frequency, $\langle U \rangle$ is the average energy density in the chamber and V is the chamber volume. It is found that [8]

$$\langle \sigma_i^{\mathrm{a}} \rangle = \frac{2\pi V}{\lambda} \frac{1}{\langle Q_i \rangle}, \tag{2}$$

where λ is the wavelength. In the steady state the power density in the chamber is constant and hence the average power absorbed by all these losses must be equal to the total power, P_1^{t}, injected into the chamber: $\langle P^{\mathrm{a}} \rangle = \langle S \rangle \sum_i \langle \sigma_i^{\mathrm{a}} \rangle = P_1^{\mathrm{t}}$. It can then be shown that, $\langle |S_{21}|^2 \rangle$, the ratio of the average received power $\langle P_2^{\mathrm{r}} \rangle$ to the transmitted power P_1^{f}, is related to the total absorption cross-section of the chamber and its contents by

$$\langle |S_{21}|^2 \rangle = \frac{\langle P_2^{\mathrm{r}} \rangle}{P_1^{\mathrm{f}}} = \eta_2^{\mathrm{T}} \frac{\lambda^2}{8\pi} \frac{1}{\langle \sigma_{\mathrm{T}}^{a} \rangle}, \tag{3}$$

where η_i^{T} are the total radiation efficiencies of the two antennas [8]. The total radiation efficiencies are given by the products of the dissipative radiation efficiencies due to ohmic and dielectric losses on the antennas (η_i^{rad}) and the reflection mismatch factors $\left(1 - \left| S_{ii}^{\mathrm{FS}} \right|^2 \right)$ of each antenna

$$\eta_i^{\mathrm{T}} = \eta_i^{\mathrm{rad}} \left(1 - \left| S_{ii}^{\mathrm{FS}} \right|^2 \right), \tag{4}$$

where S_{ii}^{FS} denotes the free-space reflection coefficient of the antennas

Since average ACS is additive within the assumptions of the ideal reverberation chamber model the ACS of the subject under test, denoted $\langle \sigma_{\mathrm{SUT}}^{\mathrm{a}} \rangle$, can be determined from two measurements of the average chamber power transmission factor $\langle |S_{21}|^2 \rangle$ with and without the subject present in the chamber with everything else left invariant [1]:

$$\langle \sigma_{\mathrm{SUT}}^{\mathrm{a}} \rangle = \frac{\lambda^2}{8\pi} \eta_1^{\mathrm{T}} \eta_2^{\mathrm{T}} \left(\frac{1}{\langle |S_{21}^{\mathrm{loaded}}|^2 \rangle} - \frac{1}{\langle |S_{21}^{\mathrm{unloaded}}|^2 \rangle} \right). \tag{5}$$

Defining the relative chamber insertion loss or *loading ratio*, by

$$L \stackrel{\mathrm{def}}{=} \frac{\langle |S_{21}^{\mathrm{unloaded}}|^2 \rangle}{\langle |S_{21}^{\mathrm{loaded}}|^2 \rangle} \geq 1 \tag{6}$$

the average ACS of the subject can also be written

$$\langle \sigma_{\mathrm{SUT}}^{\mathrm{a}} \rangle = \frac{\lambda^2}{8\pi} \eta_1^{\mathrm{T}} \eta_2^{\mathrm{T}} \frac{1}{\langle |S_{21}^{\mathrm{unloaded}}|^2 \rangle} (L - 1). \tag{7}$$

This expression is independent of the chamber volume but it does depend on the total efficiencies of the antennas. If the radiation loss efficiencies, η_i^{rad}, are known to be close to unity it may be sufficient to approximate $\eta_i^{\mathrm{T}} \approx \left(1 - \left| S_{ii}^{\mathrm{FS}} \right|^2 \right)$ and account for the approximation in the systematic uncertainty estimate. The individual total antenna efficiencies can be determined using a three-antenna method in the reverberation chamber [9]. In fact, since the average ACS only depends on the product of the efficiencies of the two antennas, a two antenna method can be used to determine this product.
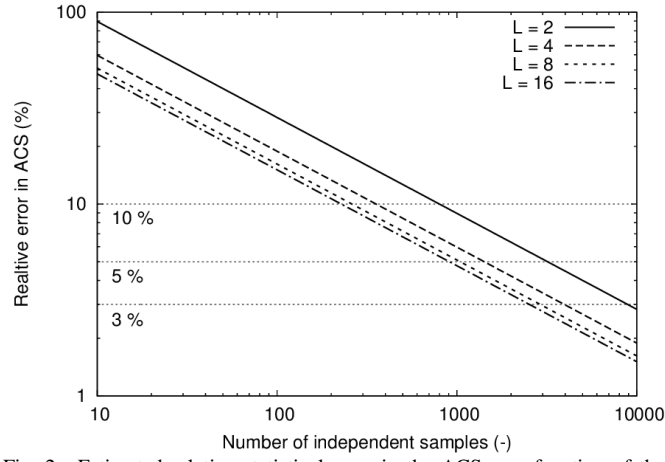
Fig. 2. Estimated relative statistical error in the ACS as a function of the number of independent samples used in the evaluation of the average chamber transmission factors for a number of chamber loading ratios.
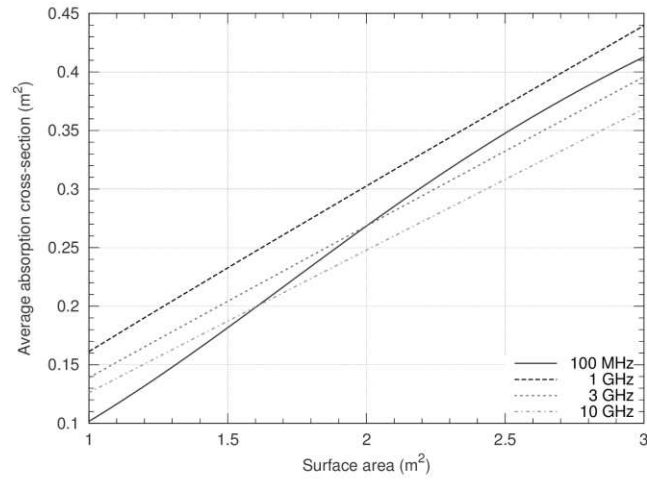

Fig. 3. Variation in the ACS of a homogeneous sphere of relative permittivity 50, conductivity 1 S m^{-1} with the surface area of the sphere.

2.2 Statistical uncertainties

The statistical uncertainty in the mean received power is given by the "standard error" of the ensemble mean of the N_{ind} independent samples of the field configurations measured. The variance of the mean received power mean is therefore related to the number of independent samples by [10]

$$\text{Var}[\langle |S_{21}|^2 \rangle] = \frac{\langle |S_{21}|^2 \rangle}{N_{\text{ind}}}. \tag{8}$$

The relative statistical uncertainty in the ACS is therefore given by [1][5]

$$\frac{\Delta \langle \sigma_{\text{SUT}}^{\text{a}} \rangle}{\langle \sigma_{\text{SUT}}^{\text{a}} \rangle} = \frac{\sqrt{2}L}{L-1} \frac{\Delta \langle |S_{21}|^2 \rangle}{\langle |S_{21}|^2 \rangle} = \frac{\sqrt{2}L}{L-1} \frac{k}{\sqrt{N_{\text{ind}}}}. \tag{9}$$

where k determines the confidence (68 % for k=1, 95 % k=2).

The variation of this relative uncertainty with the number of independent samples is shown in Fig. 2 for different chamber loading ratios. This seems to indicate that smaller uncertainties can be obtained by using a smaller chamber to give a larger loading ratio; however, the chamber must also be large enough to support sufficient cavity modes to allow enough independent samples to be obtained at the lowest frequency of the measurement. This is an important consideration for the design of a

chamber for human ACS studies.

From (2) the chamber loading ratio can be related to the unloaded quality factor of the chamber, $\langle Q_{\text{unloaded}} \rangle$, and the ACS of the subject by

$$L = 1 + \frac{\lambda \langle Q_{\text{unloaded}} \rangle}{2\pi V} \langle \sigma_{\text{SUT}}^{\text{a}} \rangle . \qquad (10)$$

This allows an estimate of the number of independent samples required to achieve a given statistical uncertainty to be made if an approximate ACS for the subject is known. The chamber used in this study has an unloaded Q-factor of 80,000 at 3 GHz and therefore the loading ratio for a subject with $\langle \sigma_{\text{SUT}}^{\text{a}} \rangle = 0.4$ m^2 is about 16.

In order to estimate the acceptable uncertainty for human ACS studies a Mie Series calculation was used to estimate the range of ACS for a body with surface area from 1 m^2 to 3 m^2 assuming a homogeneous relative permittivity of 50 and conductivity of 1 S/m [7][11]. Such simple spherical models provide a first-order estimate of absorption over a broad frequency range and are sufficiently accurate for the purpose of estimating the chamber loading ratio [12]. Previous studies have shown that human ACS correlates more strongly with body surface area (BSA) than with mass or height [13]. Fig. 3 shows that the variation of ACS with surface area is approximately linear over the physical BSA range of 1.2 m^2 to 2.5 m^2. The model suggests we need the uncertainty in the ACS to be less than 10% in order to discriminate between adults with a surface area difference of about 0.03 m^2 and an uncertainty in ACS of less than 5 % to discriminate to within about 0.01 m^2. From Fig. 2 this in turn implies the number of independent samples in the ensemble should be at least 300 for 0.03 m^2 discrimination and ideally over 800 for 0.01 m^2 discrimination, providing $L \gg 4$. Note that the uncertainty is a maximum for the smallest loading factors, i.e. for the smallest people. For children more independent samples would be needed to provide good discrimination between subjects. Simulations show a variation in ACS (for single plane-wave illumination) of 30 % between sitting and standing phantoms which we would like to be able to discriminate very easily in the measurement [14]. Considering these results a maximum statistical uncertainty of 5 % is therefore necessary in order for the measurements to clearly discriminate between different people and postures and an uncertainty of 3 % or less is desirable.

1.1. Obtaining independent field configuration samples

The most common tuning method for reverberation chambers is stepped mechanical tuning which uses one or more rotating paddle wheels to vary the boundary conditions on the fields. The ensemble average is taken over a fixed number $n = 1, \ldots, N_{\text{m}}$ of paddle angles θ_n. The paddle has to rotate through a sufficiently large angle between samples to give an independent field configuration at each position. This is normally verified by measurement of the auto-correlation function [15]. The angular movement required to reduce the autocorrelation function by a factor of $1/e$ at frequency f is denoted by $\Delta\theta_C(f)$ and is used as the metric for independent sample angles. The width of the auto-correlation function increases at low frequencies as the number of modes in the chamber decreases thus limiting the maximum number of independent samples that can be obtained. Fig. 4(a) shows the auto-correlation function at 1-8.5 GHz for the chamber used in this study. At 1 GHz there are only about 120 independent samples available from mechanical tuning whereas at 8.5 GHz over 800 are available.
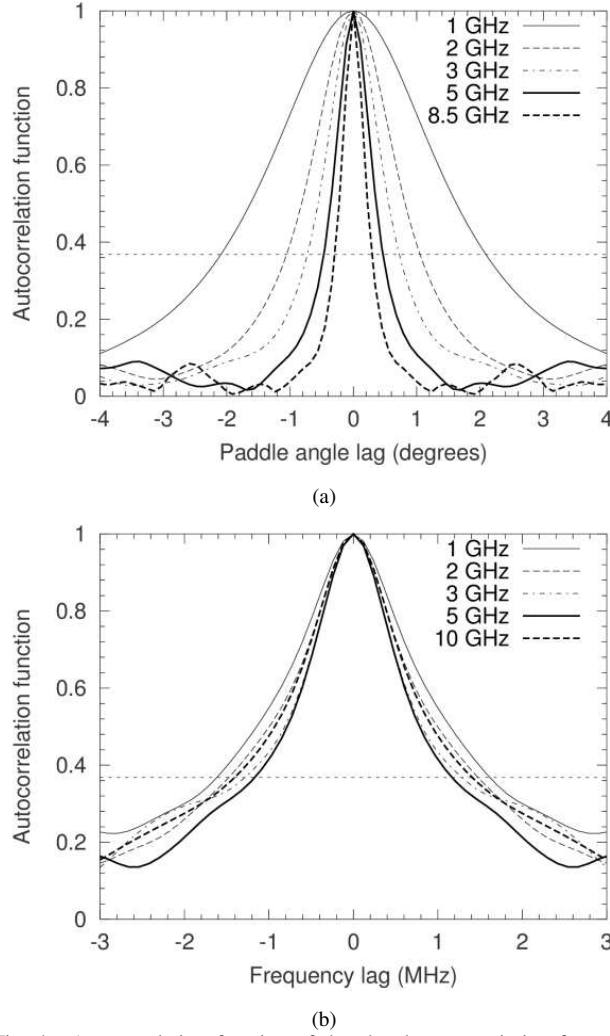
(a)

(b)

Fig. 4. Autocorrelation function of the chamber transmission factor over mechanical tuner rotation angles at various frequencies (a) and over frequency in different frequency bands (b) with a loaded chamber. The horizontal dashed line shows the 1/e metric for independent samples.

In earlier work we applied stepped mechanical tuning with 100 paddle positions to human ACS measurement; however, the measurement time was too long for subjects to reliably hold a posture and the statistical error was only 7 % [5]. A major contribution to the measurement time is the movement and damping time of the paddle between the steps. Recently it has been shown that taking frequency sweeps with a continuously rotating paddle gives the same statistical information as a stepped paddle provided that certain constraints on the measurement parameters are satisfied [16]. These constraints are that the signal sampling is large compared to the overall transient time of the chamber and measurement system and any SUT "integration times". If the VNA with intermediate frequency (IF) bandwidth Δf_{IF} collects N_{f} samples per frequency sweep in time T_{sweep} then this constraint is

$$T_{\mathrm{sweep}}/N_{\mathrm{f}} \gg \tau_{\mathrm{IF}} + \tau_{\mathrm{cables}} + \tau_{\mathrm{RC}} + \tau_{\mathrm{SUT}}, \qquad (11)$$

where $\tau_{\mathrm{IF}} \sim 1/\Delta f_{\mathrm{IF}}$ is the response time of the VNA detector, τ_{cables} is the propagation delay in the cables and $\tau_{\mathrm{RC}} \sim Q/\omega$ is the decay time of the reverberation chamber. The Joule heating response time of the subject, τ_{SUT}, is expected to be negligible compared to the other response times. The paddle should also not move significantly over the measurement time of the VNA detector implying that $2\pi/N_{\mathrm{m}}N_{\mathrm{f}} \ll \Delta\theta_{\mathrm{C}}(f)$. These constraints ultimately limit the minimum rotation period, T_{rot}, of a continuously rotating mechanical tuner. It is also shown in [16] that optimal sampling is obtained when ensemble samples are

taken at equiangular spacing of the tuner position over one full tuner rotation, with the spacing determined by the number of independent samples available within the chamber: $T_{sweep}N_m = T_{rot}$. They further demonstrated that oversampling by a factor of three is more than sufficient to collect all information within the available independent samples.

Independent field configurations can also be sampled by considering a number, N_f, of frequencies within a band around each frequency of interest [17]. The frequency spacing, Δf, in the averaging band must be large enough to give independent field configuration samples, as quantified by the 1/e half-width of the auto-correlation function with frequency, denoted by $\Delta f_C(f)$. For light loading of the chamber it can be shown that $\Delta f_C \sim f/Q(f)$ [18]. The total width of the frequency averaging band, Δf_{FS}, must not be so large that the averaging distorts any real features in the measurement. The ensemble average at each frequency in this case can be efficiently implemented using a moving average filter. Fig. 4(b) shows the auto-correlation function with frequency at a fixed paddle position in a number of frequency bands. It can be seen that the coherence bandwidth of the loaded chamber is about 1 MHz over most of the range.

2.3   Systematic uncertainties

The reverberation chamber theory above assumes that the field in the chamber is completely randomised by multiple reflections leading to phasor field components with real and imaginary parts that are distributed according to zero-mean Gaussian random processes [8]. The field is also assumed to be homogeneous, in the sense that the statistical distributions have the same variance at each location in the chamber, apart from within a quarter-wavelength of the walls [8]. Any real reverberation chamber will have some non-stochastic energy present. This non-stochastic energy can be considered as being due to so-called "direct ray paths" that do not interact with the mechanical tuning mechanism. The chamber transmission factor can in principle be decomposed into stochastic and non-stochastic parts, $S_{21} = S_{21}^s + S_{21}^{ns}$, where the vector average of the stochastic component $\langle S_{21}^s \rangle = 0$ and hence $\langle S_{21} \rangle = \langle S_{21}^{ns} \rangle$. The preponderance of non-stochastic energy is then quantified by the Rician K-factor defined by [19]

$$K = \frac{|S_{21}^{ns}|^2}{\langle |S_{21}^s|^2 \rangle} = \frac{|\langle S_{21} \rangle|^2}{\langle |S_{21} - \langle S_{21} \rangle|^2 \rangle} . \qquad (12)$$

The K-factor is not an intrinsic property of the field in the chamber, but depends on the location and orientation of the antennas and other scattering objects within the chamber. Bamba *et al.* [22] have recently discovered this effect in their "room electromagnetics" approach to in-situ exposure assessment. Table 3 in their paper indicates a systematic error in average ACS of 78% for K=-0.1 dB, 4 % for K=-6 dB and 1% for K=-10 dB.

A closely related phenomenon is that of "blocking" and backscattering of power by the SUT [20]. It has recently been shown that if either the transmitting or receiving antenna has a significant line-of-sight view of the SUT within their reception aperture then inhomogeneities are created and errors are induced in received power measurements of the reverberant field [21]. For the transmitting antenna this is caused by direct absorption of non-stochastic power, P_{SUT}^a, by the SUT and the backscattering of the non-stochastic power, P_1^a, from the SUT back into the antenna, either directly or via reflection from the chamber walls. This non-stochastic backscatter will appear as a contribution to the vector averaged reflection coefficient of the antenna, $\langle S_{11} \rangle = S_{11}^{FS} + \langle S_{11}^{ns} \rangle$, in addition to the free-space reflection coefficient. These two non-stochastic absorbed powers are not accounted for in the standard RC theory and, if present in a measurement, will lead to an over-estimation of the average ACS of the SUT since they will be taken as being absorbed by the SUT. While P_{SUT}^a is indeed absorbed by the SUT, it is not stochastic power and therefore should not be part of the average absorption cross-section; its presence will bias the average ACS in favour of the ACS as seen

TABLE I
MEASUREMENT PARAMETERS

Quantity	Symbol	Value
Frequency range	-	1-15 GHz
Number of frequency points	N_f	7000
Frequency spacing	Δf	2 MHz
Rotation period	T_{rot}	460 s
Number of sweeps	N_{sweep}	300
Sweep time	T_{sweep}	1.53 s
IF bandwidth	Δf_{IF}	100 kHz
Frequency tuning bandwidth	Δf_{FS}	100 MHz
Number of independent samples	N_{ind}	6000 at 1 GHz

from the direction of the transmitting antenna.

For the receiving antenna a related effect occurs which has been termed "blocking" [21]. An absorbing object, such as the SUT, in the aperture of the receiving antenna will block the reverberant stochastic field over a range of solid angles, reducing the received stochastic power compared to other locations in the chamber. This again can lead to an over-estimation of the average ACS of the SUT since the blocked stochastic power is interpreted as absorbed by the SUT.

The non-stochastic and reverberant behaviour can most easily be separated in the time domain where the early-time response of the power delay profile is associated with the direct non-stochastic coupling and the late time response with the diffuse stochastic coupling of the antennas [21][22]. However, such time domain measurements are too slow for human ACS measurements implemented using a VNA over a broad frequency range since they require very high frequency resolution ($\Delta f < 100$ kHz) in order to accurately extract the time decay accurately. In earlier work we subtracted out the non-stochastic part of S_{21} and considered only the stochastic part in the ACS calculation, which reduces the apparent measurement artefacts [5]. However, this cannot be rigorously justified as any non-stochastic energy at the location of the SUT cannot be assumed to be invariant with and without the SUT present in the chamber. Given the complexities and uncertainties associated with non-stochastic effects it is therefore essential to minimise both the K-factor, direct absorption of non-stochastic power by the SUT and blocking of the antennas by the SUT in any experimental arrangement by careful placement of the antennas and SUT and verification that the effects of the non-stochastic contributions are commensurate with the statistical uncertainty.

2.4   Overall experimental design

Reverberation chamber measurements using a VNA often measure full two-port scattering parameters between the two antennas. This allows the free space reflection coefficient of both antennas to the measured as $S_{11}^{FS} = \langle S_{11} \rangle$ and $S_{22}^{FS} = \langle S_{22} \rangle$ (assuming the non-stochastic power has been minimised) simultaneously with the transmission measurement. We adopted this approach in our earlier work [5]. However, the measurement time of both the empty chamber and the SUT can be halved by predetermination of the free-space reflection coefficients, since then only the transmission needs to be measured and the VNA only needs to sweep the power on one port.

As we have determined above there are only about 120 independent samples available at 1 GHz in our chamber from the mechanical tuning and this is not sufficient to give us the desired measurement uncertainty of 3 % in the average ACS. To collect the full information available from the mechanical tuner a full rotation of the tuner has to be sampled. At higher frequencies we have more than enough samples from mechanical tuning alone to obtain a statistical uncertainty of less than 3 % in the ACS. This also implies that we have to oversample at low frequencies in order to get good accuracy at higher frequencies using purely mechanical tuning in our chamber. However, at low frequencies we still need to obtain more independent samples by utilising frequency stirring.

At 1 GHz at least 50 samples per paddle angle are required from frequency tuning implying a bandwidth of $\Delta f_{FS} \gtrsim 100$ MHz

with a measurement frequency resolution of $\Delta f = 2$ MHz, a little larger than the coherence bandwidth of the chamber. This requires $N_f \gtrsim 7000$ samples per sweep to be collected for a broadband ACS measurement over 1-15 GHz. With a VNA resolution bandwidth of 100 kHz the sweep time for 7000 points is about 1.5 s, giving a total measurement time of $T_{rot} = N_m T_{sweep} \sim 450$s. The final measurement parameters for an overall subject measurement time of 460 seconds are summarised in Table I. The estimated statistical uncertainty is 3 %.

3   VALIDATION PHANTOM AND HUMAN SUBJECT

In order to validate the overall measurement procedure and the error model a spherical validation phantom was constructed. The ACS of a layered spherical phantom can be determined very accurately using a Mie Series calculation making it a suitable validation object [7]. The physical phantom consisted of an approximately spherical shell of high-density polyethylene (HDPE), with an outer diameter of 380±5 mm and thickness of 4±0.5 mm, containing de-ionised water. The error in the outer diameter includes the estimated systematic uncertainty due to the slight deviation of the phantom's shape from spherical.

The complex permittivity of HDPE is relatively frequency independent in the band 1-8.5 GHz and has little temperature dependence near room temperature [23][24]. We have therefore assumed a relative permittivity of $\varepsilon_r = 2.36\pm0.01$ and loss tangent of $\tan\delta = (120\pm10) \times 10^{-6}$ (giving an effective conductivity of $\sigma = 168\pm34$ μS m^{-1}) for the whole frequency range. The complex permittivity of water was determined from a parametric model which is accurate to within the experimental uncertainties of the underlying data (1 % for ε_r and 2 % for σ) [25]. This exhibits more temperature dependency than that of HDPE and its effect on the ACS was bounded using an ambient measurement temperature of 20±2°C.

The ACS of the spherical phantom was calculated using a Mie Series code [11]. A sensitivity analysis was performed to determine bounds on the ACS for the range of input parameter uncertainties given above.

In order to investigate the sensitivity of the measurement to variations in subject posture and clothing, the average ACS of a 26 year-old male subject of mass 72 kg and height 1.81 m was also investigated. The subject was measured wearing three different levels of clothing, and holding three different postures. Non-conductive support was provided to ensure the subject was more than a quarter-wavelength from the chamber walls, floor or ceiling in each posture.

4   RESULTS

The measured average ACS of the spherical phantom is shown in Fig. 5 compared to the results of the Mie Series calculation. Very good agreement is obtained. The dominant uncertainty (±5 %) in the Mie Series model is due to the uncertainty in the HDPE shell thickness. Confirmation of the ACS uncertainty model can be seen in Fig. 6 where the theoretical statistical uncertainty estimated from (9) is compared to the coefficient of variation of the ACS obtained over ten independent measurements of the spherical phantom. These results indicate that the ACS measurement is accurate and that the systematic uncertainty has been reduced to a level below the statistical uncertainty, except possibly above 13 GHz, where there is an increase of the coefficient of variation to about 4 %.

The average ACS of the human subject in three different postures is shown in Fig. 7. In these measurements the subject wore the same light clothing for each posture. The star posture, standing with arms and legs out-stretched, maximizes the exposed body surface area and therefore has the highest average ACS. A seated posture, with some shadowing of the arms and legs has a 4-17 % lower average ACS across the frequency range than the star posture, while the foetal posture which minimizes surface area has a 20-40 % lower average ACS than the star posture. It can be seen that the optimized measurement can easily resolve the posture dependence of the average ACS. The variability of the average ACS in the seated posture, where the subject tried to remain still in the same position and retake the same posture between measurements was also investigated. The typical variation
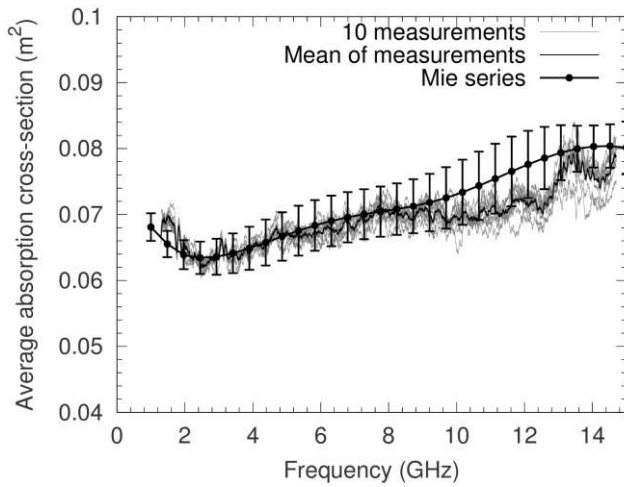
Fig. 5. Ten measurements of the ACS of the spherical phantom compared to the Mie Series calculation. The error bars on the Mie calculation results indicated the range of ACS values obtained as all the input parameters are varied over their uncertainty ranges.
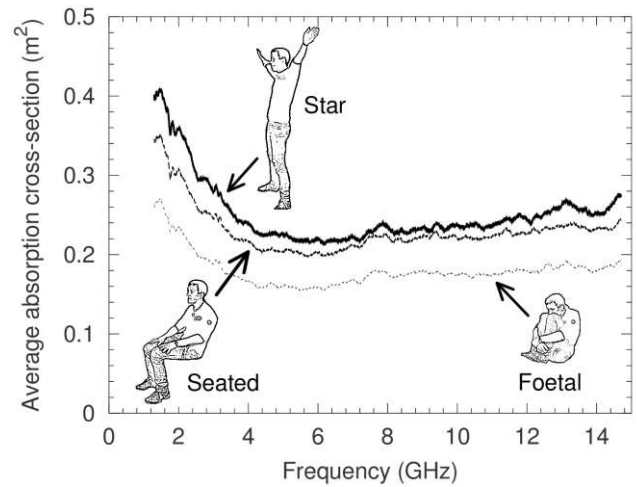

Fig.7. Measured ACS of the same human volunteer wearing light cotton clothing in three different postures.
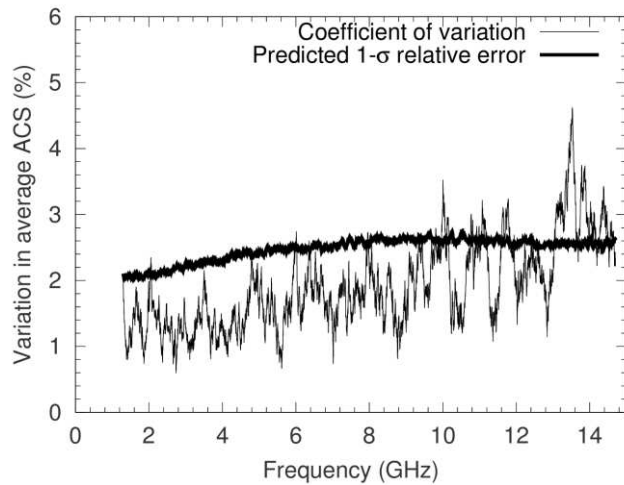

Fig. 6. Coefficient of variation of the measured ACS from 10 measurements of the spherical phantom compared to the 1-σ relative statistical uncertainty predicted by (9) using the measured loading factor.
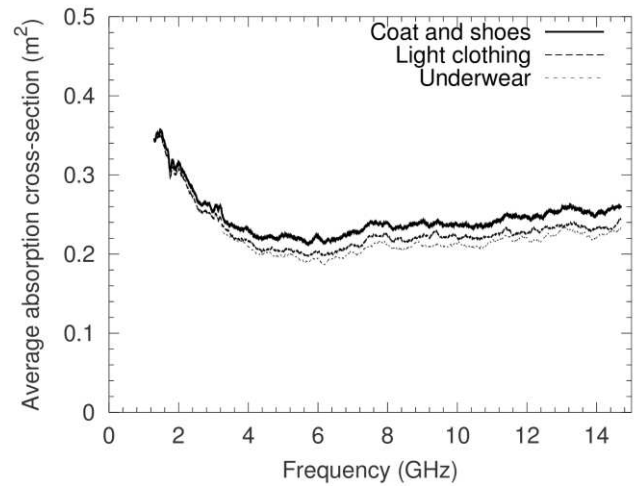

Fig. 8. Effect of clothing on the average ACS of a human volunteer in a seated posture. The subject first wore only underwear, then put on light cotton shirt, trousers and socks and then finally also put on a coat and shoes.

was found to be about 3 % which is indicative of the systematic uncertainty due to posture variation that can be expected in human ACS measurements. The measured ACS in the 1-2 GHz band is consistent with the whole-body SAR value of 0.04-0.05 W/kg with average incident power density 1 mW/cm^2 (equivalent ACS 0.29-0.37 m^2) obtained by Wang et al for a 73 kg male in a standing posture in a reverberation chamber [26]. Wang et al's results were validated against a numerical simulation of a phantom with similar physique to the measurement subject. Fig. 8 shows the average ACS of the same subject in a seated posture wearing different amounts of clothing. An increased amount of clothing increases the measured average ACS. This could be due to absorption in the clothes or it could be caused by improved impedance matching of the incident wave to the body when the clothes are present. It can be seen that light clothing increases that average ACS by no more than 5 %, which is only a little larger than the statistical uncertainty. This means that human volunteer studies can be undertaken with lightly clothed individuals with relatively low systematic error thus reducing the practical and ethical problems of measuring unclothed subjects.

5   CONCLUSIONS

An optimised experimental methodology has been developed for average ACS measurement of humans in a reverberation chamber. Using this methodology average ACS can be measured over a wide range of frequencies with a statistical uncertainty

lower than 3 % in about 8 minutes. The methodology has been validated on a spherical phantom using a Mie Series calculation. It was found to be essential to minimize systematic errors from non-stochastic couplings between the antennas and subject in order to achieve accurate results. Initial measurements of a human volunteer indicate that uncertainties due to posture changes during the measurements can be restricted to about 3%. Light clothing only introduces an uncertainty of at most +5% in the ACS allowing the possibility of accurate human studies on clothed subjects.

Reverberation chamber measurements can accurately quantify the absorption of diffuse electromagnetic fields by the human body. While the reverberation chamber measurement approach has limitations in its applicability due to the constraints of the technique it is highly complementary to the numerical simulation approach widely used in the literature for human exposure studies. The methodology reported here has subsequently been applied to a medium-scale empirical study of the variability of human exposure to electromagnetic fields due to internal and external morphological parameters [27].

REFERENCES

[1] U. Carlberg, P.-S. Kildal, A. Wolfgang, O. Sotoudeh and C. Orlenius, "Calculated and measured absorption cross sections of lossy objects in reverberation chamber," IEEE *Trans. Electromag. Compat*., vol. 46, pp. 146–154, 2004.

[2] A. Gifuni, "On the measurement of the absorption cross section and material reflectivity in a reverberation chamber," *IEEE Trans. Electromag. Compat*., vol. 51, pp. 1047-1050, 2009.

[3] J. B. Andersen, K. L. Chee, M. Jacob, G. F. Pedersen and T. Kürner, "Reverberation and absorption in an aircraft cabin with the impact of passengers," *IEEE Trans. Antennas Propagat*., vol. 60, pp. 2472–2480, 2012.

[4] A. Bamba, W. Joseph, J. B. Andersen, E. Tanghe, G. Vermeeren, D. Plets, J. Ø. Nielsen and L. Martens, "Experimental assessment of specific absorption rate using room electromagnetics," *IEEE Trans. Electromag. Compat*., vol. 54, pp. 747–757, 2012.

[5] G. C. R. Melia, M. P. Robinson, I. D. Flintoft, A. C. Marvin and J. F. Dawson, "Broadband measurement of absorption cross-section of the human body in a reverberation chamber," *IEEE Trans. Electromag. Compat.*, vol. 55, pp. 1043-1050, 2013.

[6] ICNIRP, "Guidelines for limiting exposure to time-varying electric, magnetic and electromagnetic fields (up to 300 GHz)," *Health Phys*., vol. 44, 1630–1639, 1998.

[7] C. M. Weil, "Absorption characteristics of multi-layered sphere models exposed to UHF/microwave radiation," *IEEE Trans. Biomedical Eng*., vol. 22, pp. 468-476, 1975.

[8] D. A. Hill, "Electromagnetic fields in cavities: Deterministic and statistical theories," *IEEE Press*, Piscataway, NJ, 2009.

[9] C. L. Holloway, H. A. Shah, R. J. Pirkl, W. F. Young, D. A. Hill and J. M. Ladbury, "Reverberation chamber techniques for determining the radiation and total efficiency of antennas," *IEEE Trans. Antennas. Propagat*., vol. 60, pp. 1758-1770, 2012.

[10] J. Kostas and B. Boverie, "Statistical model for a mode-stirred chamber," *IEEE Trans. Electromag. Compat*., vol. 33, pp. 366–370, 1991.

[11] P. Peña-Rodríguez, P. P. González Pérez and U. Pal U, "MieLab: A software tool to perform calculations on the scattering of electromagnetic waves by multilayered spheres," *International Journal of Spectroscopy*, vol. 2011, article 583743, 2011.

[12] O. P. Gandhi, "State of the knowledge for electromagnetic absorbed dose in man and animals," *Proc. IEEE*, vol. 68, no. 1, pp. 24-32, 1980.

[13] A. Hirata, S. Kodera, J. Wang and O. Fujiwara, "Dominant factors influencing whole-body average SAR due to far-field exposure in whole-body resonance frequency and GHz regions", Bioelectromagnetics, vol. 28, pp. 484-487, 2007.

[14] T. Nagaoka and S. Watanabe S, "Postured voxel-based human models for electromagnetic dosimetry," *Phys. Med. Biol*., vol. 53, pp. 7047-7061, 2008.

[15] X. Chen, P.-S. Kildal, C. Orlenius and J. Carlsson, "Channel sounding of loaded reverberation chamber for over-the-air testing of wireless devices: Coherence bandwidth versus average mode bandwidth and delay spread", *IEEE Antennas Wireless Propagat. Lett.*, vol. 8, pp. 678-681, 2009.

[16] V. Rajamani, C. F. Bunting and J. C. West, "Stirred-mode operation of reverberation chambers for EMC testing," *IEEE Trans. Instrum. Meas*., vol. 61, pp. 2759 – 2764, 2012.

[17] D. A. Hill, "Electronic mode stirring for reverberation chambers," *IEEE Trans. Electromag. Compat* , vol. 36, pp. 294-299, 1994.

[18] M. L. Crawford and G. H. Koepke, "Design, evaluation and use of a reverberation chamber for performing electromagnetic susceptibility/vulnerability measurements," National Bureau of Standards (NBS) , Boulder, CO, Technical Note no. 1092, 1986.

[19] C. L. Holloway, D. A. Hill, J. M. Ladbury, P. F. Wilson, G. Koepke and J. Coder, "On the use of reverberation chambers to simulate a Rician radio environment for the testing of wireless devices," *IEEE Trans. Antennas. Propagat.,* vol. 54, pp. 3167-3177, 2006.

[20] W. T. C. Burger, K. A. Remley and C. L. Holloway, "Proximity and antenna orientation effects for large-form-factor devices in a reverberation chamber," in *2013 IEEE International Symposium on Electromagn. Compat*., Denver, CO, 5-9 Aug., 2013, pp. 671-676.

[21] W. T. C. Burger, C. L. Holloway and K. A. Remley, "A proximity and orientation influence on Q-factor with respect to large-form-factor loads in a reverberation chamber," in *Proc. 2013 Int. Symp. Electromagn. Compat. (EMC Europe 2013)*, Brugge, Belgium, 2-6 Sept., 2013, pp. 369-374.

[22] A. Bamba, W. Joseph, G. Vermeeren, E. Tanghe, D. P. Gaillot, J. B. Andersen, J. Nielsen, M. Lienard and L. Martens, "Validation of experimental whole-body SAR assessment method in a complex indoor environment," *Bioelectromagnetics*, vol. 34, pp. 122-132, 2013.

[23] Electromagnetics materials measurements and applications (EMMA) club dielectric database, National Physical Laboratory, Teddington , UK, Release 1, 2000.

[24] B. Riddle, J. Baker-Jarvis and J. Krupka, "Complex permittivity measurements of common plastics over variable temperatures," *IEEE Trans. Microwave Theory Tech.*, vol. 51, pp. 727-733, 2003

[25] A. Stogryn, "Equations for calculating the dielectric constant of saline water (correspondence)," *IEEE Transactions on Microwave Theory and Techniques*, vol. 19, pp. 733-736, 1971.

[26] J. Wang, T. Suzuki, O. Fujiwara and K. Harima, "Measurement and validation of GHz-band whole-body average SAR in a human volunteer using reverbation chamber", Physics in Medicine and Biology, vol. 57, pp. 7893-7903, 2012.

[27] I. D. Flintoft, M. P. Robinson, G. C. R. Melia, J. F. Dawson and A C Marvin, "Average absorption cross-section of the human body measured at 1-12 GHz in a reverberant environment: Results of a human volunteer study", *Physics in Medicine and Biology*, vol. 59, no. 13, pp. 3297-3317, 2014.